Reprinted from Nature, Vol. 333, No. 6174, pp. 623-629, 16 June 1988

Isotope evidence of a mantle convection boundary at the Australian-Antarctic Discordance

E. M. Klein*, C. H. Langmuir*, A. Zindler*, H. Staudigel† & B. Hamelin*‡

* Lamont-Doherty Geological Observatory and Department of Geological Sciences of Columbia University, Palisades, New York 10964, USA
† Scripps Institution of Oceanography, La Jolla, California 92093, USA
‡ Laboratorie de Géochimie et Cosmochimie, 75230 Paris, France

Basalts from the Southeast Indian Ridge south of Australia form two geographically and isotopically distinct groups that show affinities with either Indian Ocean or Pacific/Atlantic Ocean isotope compositions. The data raise the possibility that there is a sharp boundary between the Indian and Pacific Ocean isotope provinces. The isotope boundary occurs over less than 200 km within the Australian-Antarctic Discordance, a tectonically complex region believed to overlie a zone of downwelling mantle flow.

THE distribution of chemical heterogeneities in the mantle and the relationship of these heterogeneities to surface features of the Earth are fundamental problems in studies of mantle dynamics. A more complete understanding of the composition and physical organization of mantle heterogeneities would place constraints on models of solid-earth geochemical cycles and the kinematics of mantle convection. Our knowledge of the identities and distribution of distinct mantle reservoirs is largely inferred from the manifestation of three-dimensional mantle variability in the two-dimensional oceanic crust. It has recently become clear that there are regionally distinct and mappable domains in the isotope composition of the oceanic crust, and the geometry of these domains can be used to characterize the distribution of sub-oceanic mantle compositions and to infer patterns of mantle flow.

One important discovery is that mid-ocean ridge basalts (MORB) from the Indian Ocean have isotope compositions that are distinct from those of Atlantic and Pacific MORB[1-12]. As the source of normal MORB is probably in the upper mantle, the existence of this large-scale, mappable, isotope unit implies that there are distinct upper mantle convection regimes that have not been homogenized by convective stirring. Little is known, however, about the location of the boundaries between these isotope domains, and how these domains and their boundaries relate to mantle convection and surficial tectonic features.

Here we present Pb, Sr and Nd isotope compositions of basalts collected along the Southeast Indian Ridge between Australia and Antarctica, and suggest that there is a remarkably abrupt eastern boundary to the Indian Ocean geochemical province. The apparent isotope boundary is located within the anomalously deep and tectonically complex Australian-Antarctic Discordance[13-15]. We then explore the significance of this boundary for models of mantle convection.

Geographic setting and sample location

The Southeast Indian Ridge (SEIR) separates the Indo-Australian and Antarctic plates (Fig. 1*a*). It extends south-east from the Indian Ocean triple junction in the central Indian Ocean, trends east-west between Australia and Antarctica, and terminates at the Macquarie triple junction in the south-west Pacific Ocean. In the region between Australia and Antarctica, both the ridge axis and its flanks are anomalously deep compared with the empirical age versus depth relation seen in other oceans[13,16]. The ridge axis reaches a depth of >4,000 m within a 500 km-wide segment of the ocean basin called the Australian-Antarctic Discordance (AAD; Figs 1*b*, 2*a*). The AAD is characterized by rough topography, low magnetic anomaly amplitudes, and a high density of north-south trending fracture zones[13-18]. Based on morphological and geophysical data, the SEIR south of Australia has been divided into three zones[14]: the ridge segments east and west of the AAD have been respectively designated as zone A and zone C; and the AAD itself as zone B (here called the AAD).

Eleven dredge hauls were made along a 1,700 km-long segment of the SEIR between 115°E and 138°E during the austral summer of 1975-76 aboard the R/V *Vema*[18] (Fig. 1*b*). Three dredge hauls were made within the AAD, five to the east within zone A, and three to the west within zone C (Figs 1*b*, 2*a*). Studies on the major-element chemistry of basalts recovered from these dredges were performed to explore the relationship between chemistry and magnetic anomaly amplitudes. We have undertaken a more extensive study of the major, trace and rare-earth element and isotope composition of samples from these dredges (ref. 19; E.M.K., C.H.L. and H.S., manuscript in preparation) and some of these results have been examined in a global context by Klein and Langmuir[20].

Anderson *et al.*[18] reported several Sr isotope analyses of whole-rock powders from these dredge hauls, but their highly radiogenic values, which approach or exceed those of sea water, suggest that these analyses suffer from the contamination problems common in whole-rock analyses of Sr isotopes. In addition, Cohen *et al.*[21] reported Pb, Sr and Nd isotope analyses of one basaltic glass from dredge D1; Hamelin *et al.*[7] described the isotope composition of this sample as that of standard MORB, contrasting it with the Indian Ocean signature. Thus, the one high-quality isotope analysis previously reported on this suite of dredge hauls suggested that the region is distinct from the Indian Ocean isotope province.

Methods

All isotope analyses were performed on natural basaltic glasses, with the exception of the Pb analysis for sample D6-1, which was performed on fresh whole-rock powder because of the paucity of glass. Glass chips were hand-picked under a binocular microscope to avoid all visible signs of alteration and to minimize the inclusion of phenocrysts. To remove possible surface contamination, samples were mildly leached for 20 min in 1 N HCl at room temperature in an ultrasonic bath, and then ultrasonically cleaned in distilled water before dissolution in HF.

For Nd, Sm, Sr and Rb analyses, ~100 mg of sample was spiked with a mixture of enriched isotopes of ^{150}Nd, ^{149}Sm, ^{84}Sr and ^{87}Rb. Chemical separation and analytical techniques used for analysis of these elements have been described by Zindler *et al.*[22]. For Pb analyses, ~300 mg of sample was dissolved and chemical separation was performed using a technique patterned after that described by Manhès *et al.*[23]. Pb separates were loaded in silica gel and H_3PO_4 onto single, zone-refined Re filaments and data were taken at several temperatures between 1,100 °C

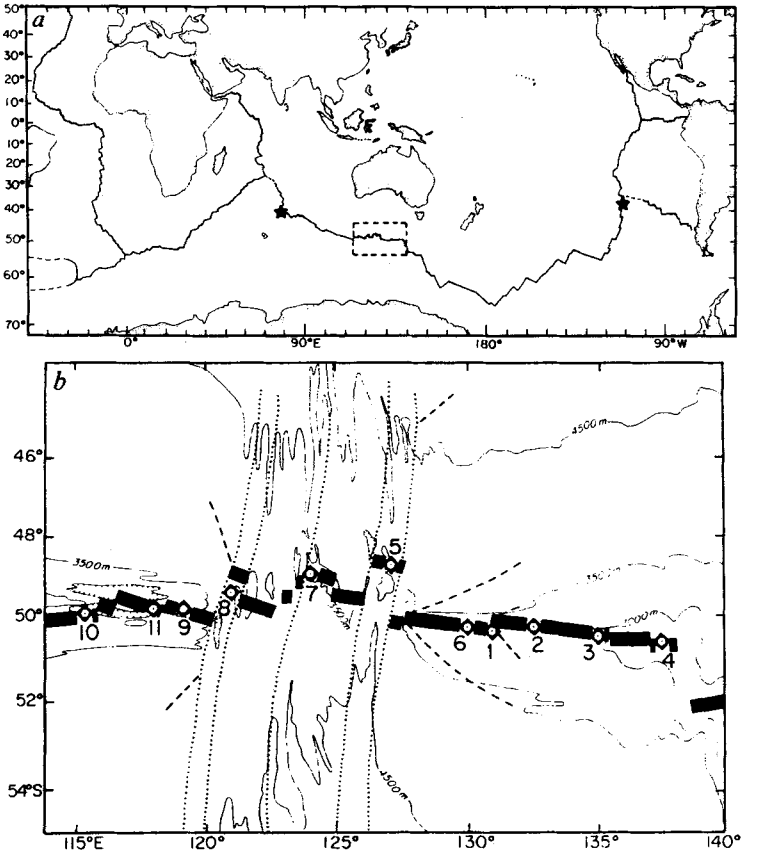

Fig. 1 *a*, Global ocean ridge system. Dashed box encompasses the area of study shown in panel *b*. Stars show locations of nearest other ridge axis samples for which isotope data are currently available[7,44]. *b*, General bathymetry and tectonic elements of the Southeast Indian Ridge, after Hayes and Conolly[13] and Vogt *et al.*[17]; 3,000 m, 3,500 m, and 4,500 m bathymetric contours are shown. Also shown are ridge segments (heavy lines), dredge locations (open diamonds), fracture zones (dotted lines) and propagating rift pseudofaults (dashed lines).

Table 1 Compositions of Southeast Indian Ridge basalts

Dredge -sample	Location	Dredge depth (m)	$^{206}Pb/^{204}Pb$	$^{207}Pb/^{204}Pb$	$^{208}Pb/^{204}Pb$	$^{87}Sr/^{86}Sr$	$^{143}Nd/^{144}Nd$	Sr	Rb	Nd	Sm
D4-1	50°12.9′ S	2,549	18.812	15.503	38.166	0.70253 ± 3	0.513139 ± 23	107	0.32	9.44	3.39
	137°33.3′ E		18.820	15.506	38.144						
D3-4	50°25.0′ S	2,910	18.998	15.613	38.468	0.70257 ± 4	0.513074 ± 19	178	0.59	12.20	3.80
	135°05.4′ E		18.959	15.566	38.363						
D2-19	50°16.0′ S	3,215	18.911	15.514	38.319	0.70261 ± 4	0.513058 ± 14	115	0.50	13.15	4.55
	132° 33.0′ E										
D1-2	50°24.5′ S	3,091	18.805	15.499	38.262	0.70264 ± 2	0.513123 ± 15	233	2.62	16.01	4.64
	131° 00.3′ E										
D6-1	50°18.0′ S	3,106	18.617	15.480	38.095	0.70259 ± 2	0.513102 ± 17	115	0.88	13.99	4.80
	130°02.5′ E										
D5-5	48°44.3′ S	4,099	18.572	15.482	38.097	0.70255 ± 3	0.513118 ± 24	131	0.52	8.58	3.00
	127°04.8′ E						*0.513108 ± 21			*8.60	
D7-3	49°02.0′ S	3,989	18.057	15.439	37.858	0.70290 ± 3	0.513037 ± 17	179	3.92	14.48	4.29
	124°00.0′ E										
D7-7	49°02.0′ S	3,989	18.008	15.462	37.794	0.70300 ± 3	0.513007 ± 21	148	1.28	7.66	2.54
	124°00.0′ E										
D8-8	49°28.0′ S	3,532	18.225	15.465	38.211	0.70314 ± 2	0.512972 ± 10	177	6.10	10.76	3.14
	121°02.0′ E		18.220	15.464	38.212						
D9-2	49°48.5′ S	3,323	18.248	15.489	38.003	0.70293 ± 3	0.513036 ± 20	124	1.19	9.06	3.08
	119° 10.5′ E										
D11-6	49°51.5′ S	3,733	17.944	15,409	37.743	0.70283 ± 3	0.513041 ± 21	145	0.75	7.49	2.54
	118°00.0′E					0.70284 ± 4		148			
D10-10	49°55.0′ S	3,087	17.772	15.494	37.837	0.70346 ± 4	0.512978 ± 14	143	1.08	7.72	2.55
	115°22.5′ E		17.756	15.472	37.768	0.70344 ± 2	0.512997 ± 20				

$^{87}Sr/^{86}Sr$ ratios are normalized to a value of 0.11940 for $^{86}Sr/^{88}Sr$ and are reported relative to a value of 0.70800 for $^{87}Sr/^{86}Sr$ for the Eimer and Amend $SrCO_3$ standard. $^{143}Nd/^{144}Nd$ ratios are normalized to a value of 0.72190 for $^{146}Nd/^{144}Nd$ and are reported relative to a value of 0.51265 for $^{143}Nd/^{144}Nd$ for BCR-1. Pb data are normalized to the values for SRM 981 reported by Hamelin *et al.*[42] (16.937, 15.491 and 36.704 for $^{206}Pb/^{204}Pb$, $^{207}Pb/^{204}Pb$ and $^{208}Pb/^{204}Pb$, respectively), which for $^{208}Pb/^{204}Pb$ differs slightly from the value reported by Catanzaro *et al.*[43]. Mean measured values of SRM 981 are 16.879 ± 0.038, 15.426 ± 0.040 and 36.512 ± 0.117 for $^{206}Pb/^{204}Pb$, $^{207}Pb/^{204}Pb$ and $^{208}Pb/^{204}Pb$, respectively (2σ; 11 runs). All reported duplicate measurements were made on separate dissolutions of the sample, with the exception of the duplicate marked by an asterisk, which was made on the same dissolution. Duplicate measurements for Pb isotope determinations agree to better than 0.05%/AMU, with the exception of the measurements for D3-4, which agree to better than 0.1%/AMU. Analytical uncertainties for Sr and Nd isotope ratios are $2\sigma/\sqrt{N}$. Blank values for Sr, Nd and Pb average 0.45, 0.07 and 0.26 ng respectively and are below the level of significance. Pb and Sr isotope analyses of D1-2 are identical within analytical uncertainty to analyses of a different sample from this dredge haul reported by Cohen *et al.*[21], these authors report a lower value of 0.51305 for $^{143}Nd/^{144}Nd$ (the reason for this difference is unclear).

and 1,200 °C. All measurements were performed on Lamont's modified V.G. Micromass 30 mass spectrometer[22].

Results

Pb, Sr and Nd isotope compositions of SEIR samples analysed in this study are presented in Table 1 and Figs 2-4. The data display substantial variations in all three systems. The SEIR data span, for example, more than half of the range in Nd-Sr isotope compositions found in MORB from the Atlantic, Pacific and Indian Oceans (Fig. 4).

In terms of along-strike systematics (Fig. 2), the data show a general trend of decreasing $^{206}Pb/^{204}Pb$ from east to west, although D7, located in the centre of the AAD, shows lower $^{206}Pb/^{204}Pb$ than both of its adjacent dredges. Sr and Nd isotopes show no gradual trends from east to west; samples from all dredge hauls east of and including D5 show lower Sr and higher Nd isotopic ratios compared with all dredges west of and including D7.

In Figs 3 and 4, our SEIR data are compared with fields for data obtained on MORB from the North Atlantic, Pacific and Indian Oceans. All samples west of and including D7 (dredges 7-11) fall within the distinct field for Indian Ocean MORB on plots of $^{206}Pb/^{204}Pb$ versus $^{208}Pb/^{204}Pb$ or $^{143}Nd/^{144}Nd$. On a plot of $^{206}Pb/^{204}Pb$ versus $^{87}Sr/^{86}Sr$, all but one sample from the western group also plot entirely within the Indian Ocean MORB field, which is characterized by high $^{87}Sr/^{86}Sr$ at low $^{206}Pb/^{204}Pb$. The exceptional sample, from dredge D10, displays even more radiogenic Sr at low values of $^{206}Pb/^{204}Pb$ than the Indian Ocean MORB field shown in Fig. 3 (note that the high $^{87}Sr/^{86}Sr$ value for this sample has been confirmed by a replicate analysis of a separate sample aliquot). In contrast, all samples east of and including D5 (dredges 1-6) fall within or close to the fields for North Atlantic and Pacific ridges on plots of $^{206}Pb/^{204}Pb$ versus $^{208}Pb/^{204}Pb$, $^{87}Sr/^{86}Sr$ or $^{143}Nd/^{144}Nd$ (Fig. 3). On a plot of $^{206}Pb/^{204}Pb$ versus $^{207}Pb/^{204}Pb$, these samples, with the exception of D3, also form a linear array that is characteristic of North Atlantic/Pacific MORB, but they are offset to lower values of $^{207}Pb/^{204}Pb$.

Thus, the SEIR data form two distinct, non-overlapping isotopic groups that correspond to longitudinal position along the ridge axis: an eastern group and a western group. Samples from the western group show strong isotopic affinities with Indian Ocean MORB, whereas samples from the eastern group show isotopic affinities with Pacific and North Atlantic MORB. The eastern group is composed of all dredges within zone A (dredges 1, 2, 3, 4 and 6) and the adjacent easternmost dredge within the AAD (dredge 5); the western group is composed of dredges 7 and 8 within the AAD and all dredges within zone C (dredges 9, 10 and 11). It should be emphasized that no sample with Pb isotope composition like any eastern group sample has yet been observed in the Indian Ocean, and conversely, no sample with Pb, Sr and Nd systematics like any western group sample has yet been observed along either the Pacific or North Atlantic Ocean ridge system.

Subtle but important differences have also been noted between the isotopic compositions of North Atlantic and Pacific MORB. White *et al.*[10] and Ito *et al.*[11] have observed that Pacific MORB show more uniform $^{87}Sr/^{86}Sr$ ratios and lower $^{143}Nd/^{144}Nd$ for the same $^{87}Sr/^{86}Sr$, compared with Atlantic MORB. Indeed, samples from the eastern group cluster on a plot of $^{87}Sr/^{86}Sr$ versus $^{143}Nd/^{144}Nd$ (Fig. 4) and extend to lower values of $^{143}Nd/^{144}Nd$ for the same $^{87}Sr/^{86}Sr$ than observed in most North Atlantic MORB. Samples from the eastern group, however, also extend to higher values of $^{206}Pb/^{204}Pb$ than N-MORB from the Pacific (Fig. 3), and do not plot entirely within the Pacific fields in Fig. 3*a-c*. Inclusion of more enriched samples from the ridges associated with the Easter microplate would expand the Pacific MORB field to these, more radiogenic values[10]. Thus, although the Pb isotopic compositions for the eastern group samples appear to be somewhat 'enriched', their Nd-Sr systematics suggest a greater isotopic affinity with Pacific MORB than with North Atlantic MORB.

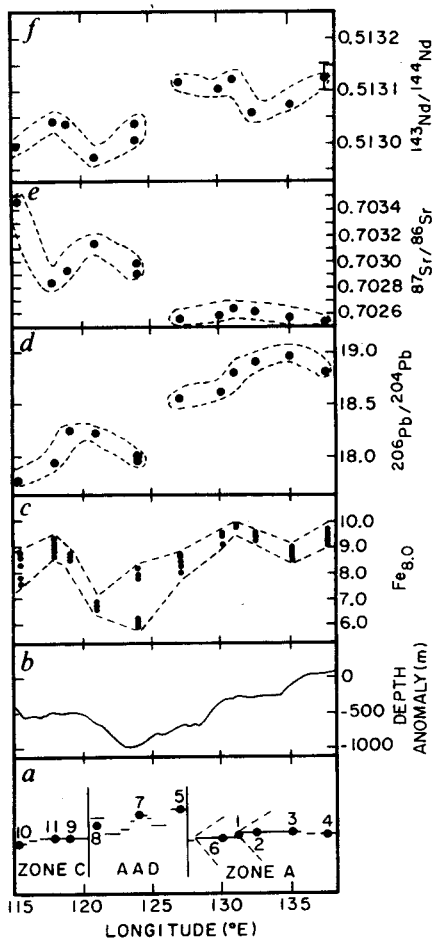

Fig. 2 Longitude (°E) versus *a*, tectonic features along the SEIR, including fracture zones bounding the AAD, propagating rifts (dashed) and dredge locations (after refs 17 and 18); *b*, depth anomalies along the ridge axis (after ref. 18); *c*, mean FeO contents of 2-13 basalts from each dredge, normalized to 8% MgO[19,20]; *d*, $^{206}Pb/^{204}Pb$; *e*, $^{87}Sr/^{86}Sr$; *f*, $^{143}Nd/^{144}Nd$. Typical analytical uncertainties ($\pm 2\sigma/\sqrt{N}$) for $^{143}Nd/^{144}Nd$ are shown by error bars on one data point; uncertainties for $^{206}Pb/^{204}Pb$ and $^{87}Sr/^{86}Sr$ are less than or equal to the size of the data points.

Discussion

The distinction in isotope composition between the western and eastern groups, and their isotope affinities with either Indian Ocean or Pacific and North Atlantic Ocean isotope compositions raise the possibility that this region forms a boundary between the Indian and Pacific Ocean isotope provinces. This hypothesis should eventually be tested by sampling of the vast unsampled or sparsely sampled segments of the adjacent SEIR and Pacific-Antarctic ridges (Fig. 1*a*). Indeed, further sampling of the Pacific-Antarctic ridge may reveal that the more radiogenic lead ratios seen in the eastern group from the SEIR are typical of the southern or eastern Pacific Ocean ridge system. The current evidence of a boundary between the Indian Ocean and Pacific Ocean isotope provinces, however, is strong enough to warrant investigation of the implications of such a boundary for mantle composition and convection.

The boundary. Our data suggest that the geographical boundary between the Indian Ocean and Pacific Ocean isotope provinces occurs between D5, which shows Pacific-like isotope compositions, and D7, which shows Indian Ocean-like compositions (Figs 2-4). Between these two dredges the ridge axis is truncated

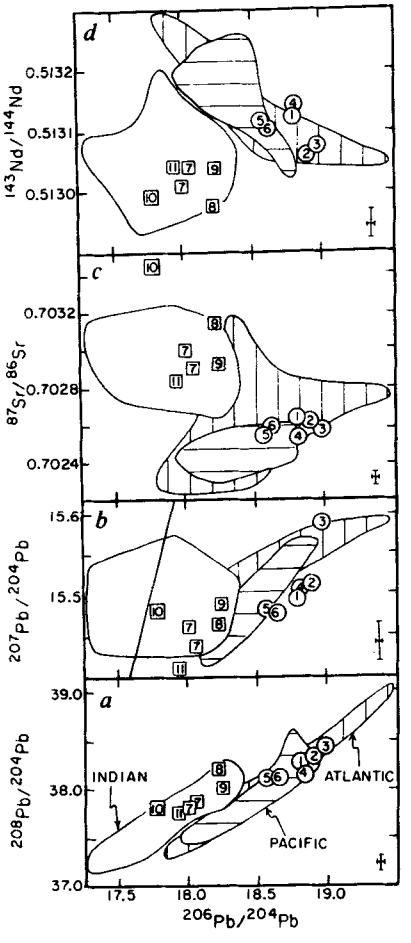

Fig. 3 $^{206}Pb/^{204}Pb$ versus *a*, $^{208}Pb/^{204}Pb$; *b*, $^{207}Pb/^{204}Pb$; *c*, $^{87}Sr/^{86}Sr$; and *d*, $^{143}Nd/^{144}Nd$. Data are plotted by dredge number: 'eastern group' sample numbers are enclosed by circles; 'western group' sample numbers are enclosed by squares. Analytical uncertainties are shown by crosses in each panel. Geochron in *b* is calculated for 4.55 Gyr, assuming initial Pb isotope composition of Canyon Diablo[45]. Fields for N-MORB isotopic data from North Atlantic (vertical ruled), Pacific (horizontal ruled), and Indian (open) Ocean ridges are shown for comparison; data for MORB fields are from refs 3–11, 21, 44, 46–48, renormalized to a comparable basis. Excluded from these N-MORB fields are samples that show the bathymetric or chemical influence of nearby hot spots (defined by criteria described by Ito *et al.*[11]). Three Indian Ocean samples with $^{87}Sr/^{86}Sr > 0.7045$ are omitted from the diagrams because they would substantially compress the $^{87}Sr/^{86}Sr$ scale[6,7]. The two samples recovered from the Sheba ridge near the Gulf of Aden[4,21] are also not included because they may be isotopically distinct from other Indian Ocean ridge volcanics[12].

by one large-offset transform (100 km) and at least one and possibly two small-offset (<30 km) transforms[17] (Fig. 1*b*). The unsampled ridge segments between these two dredges total ~200 km in length and encompass much of the eastern half of the AAD. It must be emphasized that in no place other than the AAD has a fundamental change from one MORB isotope province to another been observed. In a global context, it is thus remarkable that this change appears to occur over less than 200 km of ridge length. In the absence of sampling between dredges 5 and 7, it is not known whether this apparent isotope boundary is gradational over the intervening ridge length or occurs abruptly.

To understand the physical basis of the isotopic boundary within the AAD, it is useful to examine the geophysical information that exists for this region. One of the most striking features of this segment of the SEIR and its flanks is its anomalous depth[13,16]. On the ridge axis, the depth anomaly reaches a maximum of 1 km greater than average ridge depths in the centre of the AAD at ~124° E (the location of D7, the easternmost dredge showing Indian Ocean-like chemistry; Fig. 2). In addition, a recent analysis of Seasat altimeter data shows a pronounced, saddle-shaped, negative geoid anomaly centred on the ridge axis at ~125° E (ref. 24), and satellite gravimetry measurements show a broad, negative free-air anomaly centred on the AAD (ref. 16). Based primarily on the anomalous depth within the AAD and the associated shoaling to its east and west, Hayes and Conolly[13] and Weissel and Hayes[16] suggested that the unique bathymetry may result from downwelling convective flow within the asthenosphere, leading to a depression of mantle isotherms beneath the AAD. Thus, the AAD may represent a 'cold spot'.

Recent seismological observations are consistent with the presence of unusually cold mantle beneath the ridge axis in this region. Forsyth *et al.*[25] have reported that in the region south of Australia, Rayleigh wave phase velocities for crust <10 Myr are unusually fast beneath seafloor that shows a negative depth anomaly of more than 500 m, which includes a wide area centred on the AAD. The authors attribute these high surface wave velocities to anomalously high shear-wave velocities throughout the upper 200 km and particularly within the upper 30 km of the mantle. Similarly, global analyses of seismic wave travel-time anomalies have suggested uncommonly fast velocities at depths of 250–350 km within the mantle beneath the AAD (refs 26 and 27). These findings thus support inferences made on the basis of bathymetry that unusually cold mantle material is present beneath the region of anomalous depth centred on the AAD.

The major-element composition of these SEIR basalts also support the hypothesis that unusually cold mantle is present beneath the AAD (ref. 19; E.M.K., C.H.L. and H.S., manuscript in preparation). Klein and Langmuir[20] have suggested that regional variations in the major-element composition of basalts can be used to constrain variations in the extents and pressures of melting resulting from differences in the temperature of the sub-solidus mantle. During adiabatic upwelling, unusually cold mantle can be expected to intersect the solidus at a lower pressure and melt less upon ascent; oxides that are sensitive to the pressure of melting, such as FeO, will reflect this lower pressure of melting. Along-axis variations in FeO contents, normalized at a constant MgO content, for these SEIR basalts are shown in Fig. 2. Normalized FeO contents reach a minimum within the AAD, suggesting that these basalts are produced by lower pressures of melting, resulting from lower mantle temperatures beneath the AAD.

Implications for the plan view of mantle convection beneath the SEIR. The studies discussed above suggest that the AAD itself is anomalous compared with adjacent ridges, and our data

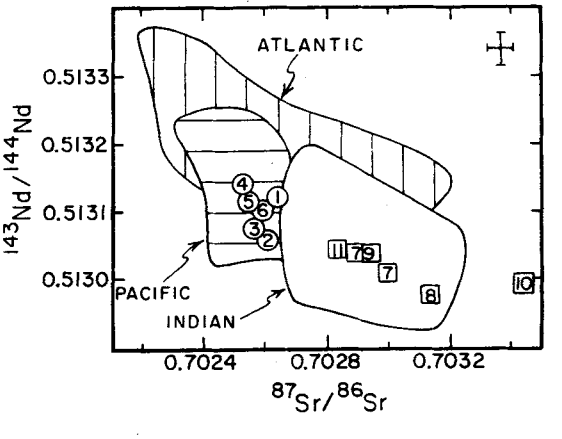

Fig. 4 $^{87}Sr/^{86}Sr$ versus $^{143}Nd/^{144}Nd$. Symbols and fields as in Fig. 3.

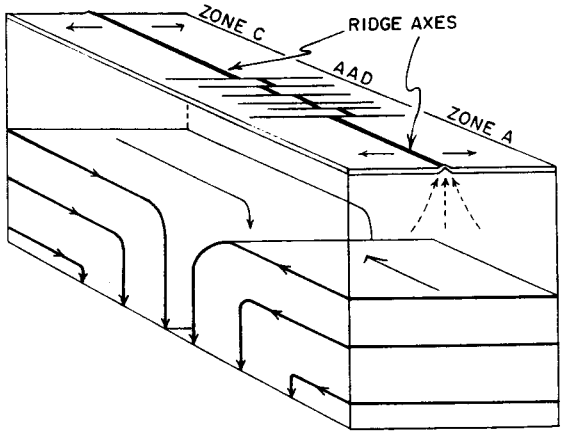

Fig. 5 Schematic model for large-scale, convective mantle downwelling beneath the AAD. Local upwelling associated with spreading of the ridge axis is indicated by the dashed arrows. See text for discussion.

suggest that a boundary between chemical provinces exists within the AAD. The question remains, then: how can a relatively sharp boundary (<200 km) between large-scale isotope provinces exist in a convecting mantle? One possible geometry might involve a 'direct convergence' pattern in which the boundary between two convective domains occurs beneath the eastern half of the AAD. In this scheme, an eastern convective domain continually feeds the Pacific Ocean isotope signature to the AAD from the east, while a western convective domain continually feeds Indian Ocean mantle to the AAD from the west. The isotope boundary would then coincide with the position along the ridge axis where the limbs of the two convective regimes converge and descend into the mantle. The descent of this material would lead to the postulated depression of mantle isotherms[16], the anomalous depth within the AAD[13] and the apparent coldness of the mantle beneath it[25]. A schematic drawing of this model of the convection pattern beneath the SEIR is shown in Fig. 5.

Independent models of global patterns of mantle or melt flow have also predicted a convergence of east- and west-flowing sub-crustal material in the basin between Australia and Antarctica. Based on the assumption that continental roots restrict upper mantle flow to sub-oceanic paths, Alvarez[28] proposed that sub-Pacific mantle flows out through three gaps, one of which occurs between Australia and Antarctica. In addition, Vogt examined global topographical gradients along ocean ridges and suggested that sub-axial asthenosphere[49] or melt[30] converges beneath topographic lows, such as the AAD. Note also that an aeromagnetic study of this region[17] has identified the presence of two active and two extinct propagating rifts converging on the AAD from the east and west.

The model of mantle flow depicted in Fig. 5 calls upon a region of deep convective downwelling beneath a ridge axis where shallow upwelling, melting and accretion associated with seafloor spreading occur. Implicit in this model is a decoupling between the geometry of flow associated with deeper convection and that associated with upwelling and melting. Although the early observations of high heat flow and shallow bathymetry at ridges fostered the assumption that ridges are underlain by hot rising jets within the mantle, more recent analyses argue against this perspective (see, for example, refs 30 and 31) and suggest that seafloor spreading in at least some areas is a passive phenomenon that draws mantle material into the zone of melting. Thus, there need be little relationship between the plan view of deeper convection and the location of the ridges; a ridge can migrate over the surface of the Earth, in response to overall plate motions and interactions, and sample mantle of the composition and temperature beneath it at any given time, which is governed by deeper convection patterns.

There is some evidence, however, for a long-lived, close spatial association between the zone of downwelling and the ridge axis within the AAD. Reviewing the data on the bathymetry of the SEIR flanks, Weissel and Hayes[16] concluded that the processes that produce the observed depth anomalies along the ridge axis have persisted for at least 30 Myr, although the locus of maximum depth has shifted a few degrees westwards with time. Furthermore, based on an analysis of sedimentary basin deposition in Australia and Antarctica, Veevers suggested that the processes responsible for the anomalous bathymetry in the region of the AAD have existed at least since the initial rifting of Australia and Antarctica during the Cretaceous[32] and possibly much longer[33]. The apparent longevity of this zone of downwelling and its association with the AAD is particularly remarkable in view of the fact that during the separation of Australia and Antarctica the ridge axis has migrated northwards more than 10° of latitude and probably eastward as well[34,35]. If, however, the zone of downwelling is a linear feature in plan view that trends roughly north-south, as we have depicted it schematically in Fig. 5, then the AAD would continually override this 'cold line' as the ridge axis migrates northward with time.

The Indian Ocean isotope province. Isotope variations in MORB have long been ascribed to mixing of ambient depleted upper mantle with one or more enriched, or less depleted, components, whose characteristics are known from the study of ocean-island basalts (see, for example, refs 36, 37). The peculiar isotopic character of both Indian Ocean MORB (Figs 3 and 4) and islands led Dupré and Allègre[5] and Hamelin *et al.*[7] to suggest that both the depleted and enriched components in the Indian Ocean are distinct in composition from those in the North Atlantic and Pacific. Hart[38] further suggested that, at least for the islands, one could define a globe-encircling band of anomalous compositions centred on 30° S latitude (the Dupal anomaly). The characteristics of this anomaly (high $^{87}Sr/^{86}Sr$, $^{207}Pb/^{204}Pb$ and $^{208}Pb/^{204}Pb$ for a given value of $^{206}Pb/^{204}Pb$) are reminiscent of an old continental source and could result from processes such as the subduction of sediment, metasomatism of the mantle wedge above a wet downgoing slab, or delamination of sub-continental lithosphere (see, for example, the discussion by Zindler and Hart[37]).

Regardless of the origin of the Dupal anomaly, it is important to note that no mixing trends have yet been observed in the Indian Ocean data set to suggest direct mixing of the hypothetical 'enriched' composition with a depleted end-member like that postulated for the North Atlantic and Pacific. This observation led Hamelin *et al.*[7] to suggest that thorough mixing in the past of the Dupal component with a depleted component like that evident in the North Atlantic and Pacific may have led to the development of a unique, depleted end-member in the upper mantle beneath the Indian Ocean. The fact that Indian Ocean MORB data do not show mixing trends emanating from a depleted composition like that seen in the North Atlantic suggests that on the scale sampled by melting, this depleted composition has been homogenized with the 'contaminant.' Thus, the apparently distinctive character of the depleted upper mantle beneath the Indian Ocean requires some mechanism that can both thoroughly contaminate the mantle beneath a large-scale region and yet maintain its convective isolation from the upper mantle beneath other ocean basins.

Our SEIR data define a geographical boundary to the Indian Ocean MORB province and, in so doing, point to an observation that may have bearing on the nature of the contamination event that produced the distinct Indian Ocean MORB signature. We note simply that all of the continents that presently circumscribe the Indian Ocean province were assembled and moved approximately as a unit, Gondwanaland, throughout the Palaeozoic. Thus, if upper mantle convection beneath these continental land masses was decoupled from the larger global convection patterns, and if contamination by delamination or subduction

occurred during that time, then a mechanism for the production of a distinct Indian Ocean 'depleted' (but contaminated) MORB reservoir is possible. The sharp isotope boundary within the AAD is comprehensible from this perspective: in contrast to the separation of India and Africa from Antarctica, which in plan view opened an 'internal' ocean basin surrounded by Gondwanaland continents, the separation of Australia from Antarctica opened a pathway from the Pacific province to the mantle beneath the Gondwanaland continents (see, for example, refs 34 and 35). Indeed, if convection within the Pacific Ocean mantle is bounded by continental roots[28] or subduction zones, then the region between Australia and Antarctica represents one of the few apparently unobstructed pathways for communication between Pacific and Indian Ocean (sub-Gondwanaland) convective regimes.

The existence of an eastern boundary to the Indian Ocean isotope province raises an obvious question concerning a possible western boundary. The location and characteristics of a western boundary, however, are not yet clear[7]. On Pb–Pb variation diagrams, some of the data of Hanan *et al.*[39] for the southern mid-Atlantic ridge significantly increase the degree of overlap between the the fields for the Indian and Atlantic/Pacific Ocean MORB isotopic provinces. The distinctive compositions of these ridge axis samples, however, appear to be due to the influence of the nearby islands of Tristan da Cunha, Gough and the Discovery Tablemount which show the Dupal isotope signature. Pb isotope data are not available for the ridge segments east and west of the Bouvet triple junction in the South Atlantic, although samples from these ridges display Nd and Sr isotopic systematics that differ somewhat from those seen in the North Atlantic and, in addition, show trace element affinities with Indian Ocean MORB (refs 40 and 41). It is possible, therefore, that further sampling and analysis will extend the Indian Ocean MORB isotope province to the mantle beneath the South Atlantic. Indeed, this would support the observation made above regarding the possible insulation of sub-Gondwanaland mantle from external convective regimes, since South America and Africa, too, were united throughout the Palaeozoic. Like the breakup of Australia and Antarctica, the separation of Africa from South America opened a channel for communication with the sub-Gondwanaland upper mantle, and with time for convective mixing we might expect to see a mixture of the two MORB isotope signatures in the South Atlantic.

Conclusions

Pb, Sr and Nd isotope compositions of basalts collected along the Southeast Indian Ridge (115° E–138° E) show considerable variations but, to first-order, form two distinct isotope groups that correspond to longitudinal position along the ridge axis. Samples from the western group show isotope characteristics commonly associated with Indian Ocean MORB whereas samples from the eastern group show isotopic affinities with North Atlantic/Pacific MORB. Based on these affinities and on proximity to either the Indian or Pacific Ocean ridge systems, we suggest that a fundamental boundary between different isotope provinces occurs beneath the Australian–Antarctic Discordance, a region of the seafloor which may overlie a zone of downwelling convective flow. We propose that the isotope boundary also results from the convergence of convective flow in which Indian Ocean-type mantle is continually fed to the AAD from the west and Pacific Ocean-type mantle is fed to the AAD from the east.

The authors thank D. Walker, D. Christie, J. Rubenstone, J. Mahoney, A. P. LeHuray, K.-H. Park, H. Brueckner, T. Plank, J. Weissel, R. Buck and N. Bogen for criticizing the manuscript. We also thank the scientific party and crew of R/V *Vema*, cruise 33, legs 1 and 2 for collecting samples. Supported by the National Science Foundation (C.H.L., A.Z., H.S., and L-DGO Deep Sea Sample Repository) and the Office of Naval Research (L-DGO DSSR). L-DGO Contribution number 4308.

Received 8 January; accepted 28 April 1988.

1. Subbarao, K. V. & Hedge, C. E. *Earth planet. Sci. Lett.* **18**, 223-228 (1973).
2. Hedge, C. E., Futa, K., Engel, C. G. & Fisher, R. L. *Contr. Miner. Petrol.* **68**, 373-376 (1979).
3. Sun, S.-S. *Phil. Trans. R. Soc.* **A297**, 409-445 (1980).
4. Cohen, R. S. & O'Nions, R. K. *J. Petrology* **23**, 299-324 (1982).
5. Dupré, B. & Allègre, C. J. *Nature* **303**, 142-146 (1983).
6. Hamelin, B. & Allègre, C. J. *Nature* **315**, 196-199 (1985).
7. Hamelin, B., Dupré, B. & Allègre, C. J. *Earth planet. Sci. Lett.* **76**, 288-298 (1986).
8. Price, R. C., Kennedy, A. K., Riggs-Sneeringer, M. & Frey, F. A. *Earth planet. Sci. Lett.* **78**, 379-396 (1986).
9. Michard, A., Montigny, R. & Schlich, R. *Earth planet. Sci. Lett.* **78**, 104-114 (1986).
10. White, W. M., Hofmann, A. W. & Puchelt, H. *J. geophys. Res.* **92**, 4881-4893 (1987).
11. Ito, E., White, W. M. & Göpel, C. *Chem. Geol.* **62**, 157-176 (1987).
12. Mahoney, J. J. *et al. J. geophys. Res.* (submitted).
13. Hayes, D. E. & Conolly, J. R. in *Antarctic Oceanology II: the Australian-New Zealand Sector, Antarctic Res. Ser. vol. 19* (ed. Hayes, D. E.) 125-145 (Amer. Geophys. Union, Washington, D. C., 1972).
14. Weissel, J. K. & Hayes, D. E. *Nature* **213**, 518-521 (1971).
15. Weissel, J. K. & Hayes, D. E. in *Antarctic Oceanology II: the Australian-New Zealand Sector, Antarctic Res. Ser. Vol. 19* (ed. Hayes, D. E.) 165-196 (Amer. Geophys. Union, Washington, DC, 1972).
16. Weissel J. K. & Hayes, D. E. *J. geophys. Res.* **79**, 2579-2587 (1974).
17. Vogt, P. R., Cherkis, N. Z. & Morgan, G. A. in *Antarctic Earth Science* (eds Oliver, R. L., James, P. R. & Jago, J. B.) 608-613 (Australian Academy of Science, Canberra, 1983).
18. Anderson, R. N., Spariosu, D. J., Weissel, J. K. & Hayes, D. E. *J. geophys. Res.* **85**, 3883-3898 (1980).
19. Klein, E. M., Langmuir, C. H., Zindler, A. & Staudigel, H. *Trans. Am. geophys. Un.* **65**, 301 (1984).
20. Klein, E. M. & Langmuir, C. H. *J. geophys. Res.* **92**, 8089-8115 (1987).
21. Cohen, R. S., Evensen, N. M., Hamilton, P. J. & O'Nions, R. K. *Nature* **283**, 149-153 (1980).
22. Zindler, A., Staudigel, H. & Batiza, R. *Earth planet. Sci. Lett.* **70**, 175-195 (1984).
23. Manhès, G., Minster, J. F. & Allègre, C. J. *Earth planet. Sci. Lett.* **39**, 14-24 (1978).
24. Marsh, J. G., Brenner, A. C., Beckley, B. D. & Martin, T. V. *J. geophys. Res.* **91**, 3501-3506 (1986).
25. Forsyth, D. W., Ehrenbard, R. L. & Chapin, S. *Earth planet. Sci. Lett.* **84**, 471-478 (1987).
26. Dziewonski, A. M. & Anderson, D. L. *Am. Scient.* **72**, 483-494 (1984).
27. Woodhouse, J. H. & Dziewonski, A. M. *J. geophys. Res.* **89**, 5953-5986 (1984).
28. Alvarez, W. *J. geophys. Res.* **87**, 6697-6710 (1982).
29. Vogt, P. R. *Earth planet. Sci. Lett.* **29**, 309-325 (1976).
30. Houseman, G. A. *Earth planet. Sci. Lett.* **64**, 283-294 (1983).
31. McKenzie, D. & Bickle, M. J. *J. Petrology* (in the press).
32. Cande, S. C. & Mutter, J. C. *Earth planet. Sci. Lett.* **58**, 151-160 (1982).
33. Veevers, J. J. *Nature* **295**, 315-317 (1982).
34. Norton, I. O. & Sclater, J. G. *J. geophys. Res.* **84**, 6803-6830 (1979).
35. Morgan, W. J. in *The Sea* Vol. 7 (ed. Emiliani, C.) 443-487 (Wiley, New York, 1981).
36. Schilling, J.-G. *Nature* **242**, 565-571 (1973).
37. Zindler, A. & Hart, S. *A. Rev. Earth. planet. Sci.* **14**, 493-571 (1986).
38. Hart, S. R. *Nature* **309**, 753-757 (1984).
39. Hanan, B. B., Kingsley, R. H. & Schilling, J.-G. *Nature* **322**, 137-144 (1986).
40. le Roex, A. P. *et al. J. Petrology* **24**, 267-318 (1983).
41. le Roex, A. P. *et al. Contr. Miner. Petrol.* **90**, 367-380 (1985).
42. Hamelin, B., Manhès, G., Albarede, F. & Allègre, C. J. *Geochim. cosmochim. Acta* **49**, 173-182 (1985).
43. Catanzaro, E. J., Murphy, T. J., Shields, W. R. & Garner, E. L. *J. Res. nat. Bur. Stand.* **72A**, (1968).
44. Macdougall, J. D. & Lugmair, G. W. *Nature* **313**, 209-211 (1985).
45. Tatsumoto, M., Knight, R. J. & Allègre C. J. *Science* **180**, 1279-1283 (1973).
46. Hamelin, B., Dupré, B. & Allègre, C. J. *Earth planet. Sci. Lett.* **67**, 340-350 (1984).
47. Macdougall, J. D. & Lugmair, G. W. *Earth planet. Sci. Lett.* **77**, 273-284 (1986).
48. Machado, N., Ludden, J. N., Brooks, C. & Thompson, G. *Nature* **295**, 226-228 (1982).
49. Vogt, R. R. & Johnson, G. L. *Earth planet. Sci. Lett.* **18**, 49-58 (1973).